MECHANISMS OF FAULTING IN AND AROUND CALORIS BASIN, MERCURY. Andrew M. Freed[1], Sean C. Solomon[2], and Patrick J. Kenedy[1], [1]Department of Earth and Atmospheric Sciences, Purdue University, West Lafayette, IN, USA, freed@purdue.edu; [2]Department of Terrestrial Magnetism, Carnegie Institution of Washington, Washington, DC, USA.

Introduction: An important aspect of the early evolution of a terrestrial planet is the thermal and mechanical development of the lithosphere, as revealed by its response to various forms of loading. Whereas the evidence regarding the nature of the early lithosphere has long since been removed on Earth and Venus, Mercury's heavily cratered surface appears to have experienced comparatively little volcanic resurfacing or tectonic activity since the end of heavy bombardment (~3.8 Ga) [1,2]. The Caloris basin, at 1300 km in diameter [3] one of the largest and youngest impact basins on Mercury, preserves an extensive pattern of faulting that provides important clues to the manner by which Mercury's early lithosphere responded to basin formation and to subsequent lithospheric loading.

The Caloris basin is extensively fractured, with contractional ridges found over much of the basin floor, most prominently in an arc extending from ~430 to ~600 km from the basin center [4]. Fault patterns in the innermost regions of the Caloris floor are not well constrained, because when Mariner 10 imaged Caloris the dawn terminator was approximately 200 km east of the basin center and the central basin floor was not illuminated. These ridges are considered analogous to those found within lunar mascon mare basins, which formed when uncompensated mare basalt fill induced lithospheric subsidence that resulted in horizontal compressional stresses, contractional strain, and near-surface faulting. At some point, the stress state within the Caloris basin changed from compressional to extensional, as numerous extensional troughs cross-cut the ridges and are therefore younger [4-6]. These troughs have been interpreted to be graben as much as 10 km wide and are concentrated in a broad arc that extends from ~200 to ~470 km from the basin center [7]. As with the ridges, it is not known whether these graben extend inward of 200 km radial distance.

The region outside the Caloris basin is covered by hummocky plains, interpreted to be ejecta, and more extensive smooth plains, interpreted to be either fluidized impact ejecta or volcanic deposits. The exterior plains are extensively cut by contractional features (wrinkle ridges and scarps) oriented both radially and concentric to the basin rim [4], though most such tectonic features are basin concentric [5]. Basin-concentric wrinkle ridges well outside the impact basin on the Moon are thought to represent a response to some combination of basin loading at a time when cooling of the mantle had led to a thicker (>100 km) mechanical lithosphere and superposed compressive stress from global contraction [8-11]. Plains external to the Caloris basin, however, may have themselves exerted a strong influence on local or regional flexure if emplaced in deposits of sufficient thickness [6], as suggested by topographic profiles across low-latitude exterior plains units obtained by Earth-based radar [12]. A contribution from global contraction may also have been important.

The style and distribution of faulting in and around the Caloris basin can be applied as constraints on numerical simulations of the response of Mercury's lithosphere to an evolving combination of volcanic and global contractional loading. Here we use axisymmetric viscoelastic finite element models to understand how styles of faulting are influenced by assumptions regarding the shape of the Caloris basin floor, the magnitude of interior and exterior loads, the thickness of the lithosphere, the strength of surface rocks, and the viscosity structure of the interior. We also test two of the mechanisms proposed to explain later-stage extensional features on the Caloris basin floor [6,7].

Results: The models support the inference that contractional features on the Caloris basin floor are consistent with subsidence associated with a flexural response to partial basin infilling by smooth plains deposits, presumed to be volcanic in origin (Figure 1a). Models that account for the locations of contractional features near the edges of the basin floor involve fill that is of nearly uniform thickness over most of the basin (out to 500 km or greater distance from the basin center). This result suggests that the pre-fill Caloris basin floor was flatter than the geometry that has been inferred for similar sized basins on the Moon. A variety of fill thicknesses, emplacement scenarios, and lithospheric thicknesses lead to interior thrust faulting associated with subsidence. The observed distribution of contractional features is best matched by comparatively large values of fill thickness (several kilometers or more) but provides little constraint on lithospheric thickness.

A later stage of normal faulting within the basin interior can be explained by the emplacement of exterior smooth plains within an annular zone that extends from 1 to 3 basin radii (750 to 1800 km) from the basin center [6] (Figure 1b). In order that flexural uplift within the basin induced by this external load modified the stress field beneath the basin floor from a state of compression to one of net extension, the external load must have been relatively thick (5 km or more). In addition, infilling of the basin floor must have occurred in stages spaced over a time frame longer than the timescale for basin subsidence in response to a single interior load, so as to reduce the early compressive stresses in the uppermost layer of basin-floor fill. Calculations show that later-stage flow of a viscous layer at the base of the crust can induce uplift of the basin

[7], but not net extension, as early-stage compressive stresses associated with basin subsidence are too great to be overcome. If initial compressive stresses were completely relieved by thrust faulting, then a later-stage inward flow of the lower crust could, under some conditions, induce extension in the basin, though still not in a manner consistent with the observed distribution of normal faulting. Thrust faulting observed on exterior smooth plains can be the result of local loading-induced subsidence, again if these plains are relatively thick, but any constraint on the thickness of annular smooth plains from the distribution of exterior ridges can be substantially relaxed if significant compressional stresses associated with global contraction were superimposed.

The results of this analysis demonstrate that three of the most important factors that influenced faulting in and around the Caloris basin were the thickness and distribution of fill within the basin, the thickness of the exterior smooth plains deposits, and the amount of stress relief within the basin that accompanied early-stage thrust faulting. The MESSENGER mission will provide measurements of topography, gravity, and detailed fault characteristics that should substantially improve constraints on all of these factors, an outcome that will strengthen the importance of the Caloris basin as a laboratory for understanding interior heat flow, magmatism, and deformation during Mercury's early history.

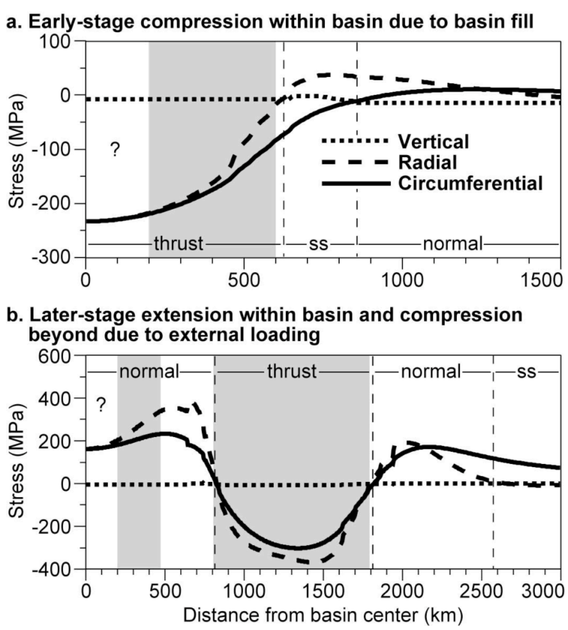

Figure 1. (a) Calculated principal stresses as functions of distance from the center of Caloris after partial basin infilling and subsidence. Negative stresses are compressive. Predicted styles of faulting based on the relative magnitude of principal stresses are noted. The gray region shows where early-stage thrust faulting in the Caloris basin is observed. The question mark in the innermost basin denotes that the nature of faulting within this region is not known. (b) Principal stresses after placement and subsidence of external smooth planes. The gray regions show where later-stage extensional faulting in the Caloris basin and compressional faulting outside are observed.

What will MESSENGER find?: Our models make several predictions for what MESSENGER may find. The models predict that the interior 200 km of the basin, which was not imaged by Mariner 10, should be pervasively faulted with both compressional and extensional features. In most of our faulting scenarios, this region experiences the highest level of differential stresses. An innermost region not pervasively faulted, however, would point to a relatively thin (<50 km) lithosphere at the time of load emplacements; to a basin floor that is not deepest near the center; or to the presence of a relatively thin, late-stage surficial layer sufficiently thick to bury earlier faults but not so thick as to induce significant subsidence.

Our results also have implications for measurements of Mercury's gravity field to be obtained by MESSENGER. Because the models suggest that the formation of later-stage normal faults within the Caloris basin floor reflect primarily the near-surface stress state within only a surficial layer of fill material, the net displacement of the basin floor after all loading processes were completed was one of subsidence. If the freshly formed basin achieved a state of isostatic equilibrium prior to initial infilling, the Caloris basin interior should be the site of a positive free air gravity anomaly, i.e., a mascon. This inference is in contrast to the prediction [13] that interior uplift should not occur if the basin floor has a net positive gravity anomaly. If interior uplift was the result of loading by exterior plains deposits, then basin floor uplift could have occurred even if the basin is a mascon. As predicted [13], the exterior deposits should also be sites of positive gravity anomalies. The overall gravity anomaly associated with the basin and its surroundings might therefore be approximately that of a bull's-eye, with a central positive anomaly surrounded by a positive annulus separated from the central anomaly by a ring of lower gravity. The actual pattern, of course, is likely to more complicated, reflecting departures from early local isostasy and uneven emplacement of plains deposits.

References: [1] Spudis, P. D., and J. E. Guest (1988), in *Mercury*, U. Ariz. Press, Tucson, pp. 118-164. [2]. Solomon, S. C. (2003), *EPSL, 216*, 441-455. [3] Pike, R. J. (1988) in *Mercury*, U. Ariz. Press, Tucson, pp. 165-273. [4] Strom, R. G., N. J. Trask, and J. E. Guest (1975) *JGR, 80*, 2748-2507. [5] Dzurisin, D. (1978), *JGR*, *83*, 4883-4906. [6] Melosh, H. J., and W. B. McKinnon (1988) in *Mercury*, U. Ariz. Press, Tucson, pp. 374-400. [7] Watters, T. R., F. Nimmo, and M. S. Robinson (2005) *Geology, 33*, 669-672. [8] Phillips, R. J., J. E. Conel, E. A. Abbott, W. L. Sjogren, and J. G. Morton (1972) *JGR, 77*, 7106-7114. [9] Solomon, S. C., and J. W. Head (1979) *JGR, 84*, 1667-1682. [10] Solomon, S. C., and J. W. Head (1980) *Rev. Geophys., 18*, 107-141. [11] Freed, A. M., H. J. Melosh, and S. C. Solomon (2001) *JGR, 106*, 20,603-20,620. [12] Harmon, J. K., D. B. Campbell, D. L. Bindschadler, J. W. Head, and I. I. Shapiro (1986) *JGR, 91*, 385-401. [13] Melosh, H. J., and D. Dzurisin (1978) *Icarus, 33*, 141-144.